MOLECULAR ECOLOGY

Molecular Ecology (2014) **23**, 4813–4830 doi: 10.1111/mec.12898

Range-wide multilocus phylogeography of the red fox reveals ancient continental divergence, minimal genomic exchange and distinct demographic histories

MARK J. STATHAM,* JAMES MURDOCH,† JAN JANECKA,‡ KEITH B. AUBRY,§ CEIRIDWEN J. EDWARDS,¶ CARL D. SOULSBURY,** OLIVER BERRY,†† ‡‡ ZHENGHUAN WANG,§§ DAVID HARRISON,¶¶ MALCOLM PEARCH,¶¶ LOUISE TOMSETT,*** JUDITH CHUPASKO††† and BENJAMIN N. SACKS*‡‡‡

**Mammalian Ecology and Conservation Unit, Veterinary Genetics Laboratory, University of California, One Shields Avenue/Old Davis Road, Davis, CA, 95616-8744, USA, †Rubenstein School of Environment and Natural Resources, 303A Aiken Center, University of Vermont, 81 Carrigan Drive, Burlington, VT, 05405, USA, ‡Department of Biological Sciences, Duquesne University, 600 Forbes Avenue, Pittsburgh, PA, 15282, USA, §U.S. Forest Service, Pacific Northwest Research Station, Olympia, WA, 98512, USA, ¶Research Laboratory for Archaeology, University of Oxford, Dyson Perrins Building, South Parks Road, Oxford, OX1 3QY, UK, **School of Life Sciences, University of Lincoln, Brayford Pool, Lincoln, LN6 7TS, UK, ††CSIRO Marine and Atmospheric Research, Centre for Environment and Life Sciences, Floreat, WA, 6014, Australia, ‡‡Invasive Animals Cooperative Research Centre, School of Animal Biology (M092), The University of Western Australia, Crawley, WA, 6009, Australia, §§School of Life Sciences, East China Normal University, No. 3663, North Zhongshan Road, 200062, Shanghai, China, ¶¶Harrison Institute, Bowerwood House, 15, St. Botolph's Road, Sevenoaks, Kent, TN13 3AQ, UK, ***Mammal Section, Department of Life Sciences, The Natural History Museum, Cromwell Road, London, SW7 5BD, UK, †††Mammalogy Department, Harvard Museum of Comparative Zoology, 52 Oxford Street, Cambridge, MA, 02138, USA, ‡‡‡Department of Population Health and Reproduction, University of California, One Shields Avenue/Old Davis Road, Davis, CA, 95616-8744, USA*

Abstract

Widely distributed taxa provide an opportunity to compare biogeographic responses to climatic fluctuations on multiple continents and to investigate speciation. We conducted the most geographically and genomically comprehensive study to date of the red fox (*Vulpes vulpes*), the world's most widely distributed wild terrestrial carnivore. Analyses of 697 bp of mitochondrial sequence in ~1000 individuals suggested an ancient Middle Eastern origin for all extant red foxes and a 400 kya (SD = 139 kya) origin of the primary North American (Nearctic) clade. Demographic analyses indicated a major expansion in Eurasia during the last glaciation (~50 kya), coinciding with a previously described secondary transfer of a single matriline (Holarctic) to North America. In contrast, North American matrilines (including the transferred portion of Holarctic clade) exhibited no signatures of expansion until the end of the Pleistocene (~12 kya). Analyses of 11 autosomal loci from a subset of foxes supported the colonization time frame suggested by mtDNA (and the fossil record) but, in contrast, reflected no detectable secondary transfer, resulting in the most fundamental genomic division of red foxes at the Bering Strait. Endemic continental Y-chromosome clades further supported this pattern. Thus, intercontinental genomic exchange was overall very limited, consistent with long-term reproductive isolation since the initial colonization of North America. Based on continental divergence times in other carnivoran species pairs, our findings support a model of peripatric speciation and are consistent with the previous classification of the North American red fox as a distinct species, *V. fulva*.

Correspondence: Mark J. Statham, Fax: +1 530 752 3556;
E-mail: Statham@ucdavis.edu

Keywords: global phylogeography, mitochondrial DNA, nuclear DNA, Pleistocene, speciation, *Vulpes fulva*, *Vulpes vulpes*, Y-chromosome

Received 21 August 2013; revision received 19 August 2014; accepted 20 August 2014

Introduction

Climatic fluctuations of the Quaternary Period shaped the evolutionary histories of many terrestrial taxa (Hewitt 2000; Lessa *et al.* 2003). In the Northern Hemisphere, many temperate taxa responded to cyclical climatic changes by range expansions during interstadial periods that enhanced population connectivity, followed by range contractions during glacial periods that reduced connectivity and resulted in population fragmentation. The corresponding fluctuations in sea level periodically uncovered overland colonization routes between landmasses that would otherwise have been isolated from one another. This repeated process of colonization and isolation produced many geographically restricted lineages, which diverged through random genetic drift or natural selection, often paving the way for speciation (Hewitt 2000). Although the impacts of glaciations probably varied throughout the Northern Hemisphere, a general pattern of 'southern richness and northern purity' has been described (Hewitt 1999; p. 106). This phrase refers to a common biogeographic pattern that originated at the end of the Pleistocene (~11.7 kya), whereby the northern portions of many species' ranges were colonized by limited subsets of species' diversity, while southern areas maintained both higher diversity and divergent ancestral lineages (Hewitt 2000; Leonard *et al.* 2005; Korsten *et al.* 2009). Populations that diverged earlier in the Pleistocene and have endured subsequent glacial cycles are the ones most likely to have led to recent species-level evolutionary divergence (Hewitt 2000).

Molecular investigations have been pivotal in building a broad understanding of Pleistocene histories. Widely distributed generalist taxa can provide insights into biogeographic processes on an intercontinental scale; however, few phylogeographic studies have sampled the ranges or genomes of such taxa sufficiently to generate a comprehensive understanding of their evolutionary history (but see Culver *et al.* 2000). While regional studies, especially those based on mitochondrial sequences, can be informative in narrower contexts, reaching higher-order phylogenetic conclusions from inadequately sampled ranges and genomes can lead to misconceptions that are difficult to dispel, even after contradictory data have accumulated (Randi 2010; Hailer *et al.* 2012; Shrotriya 2012). For example, initial genetic studies of grey wolves (*Canis lupus*) in both Eurasia and North America emphasized northern populations and indicated a relatively homogeneous Holarctic population derived from post-Pleistocene range expansions (Vila *et al.* 1999). Subsequent analyses in areas of biogeographic complexity, including southern portions of the species' range, found higher diversity and significant divergence dating to the mid-Pleistocene (Sharma *et al.* 2004; Leonard *et al.* 2005; Weckworth *et al.* 2010) and in other cases blurred lines between previously accepted *Canis* species (Wilson *et al.* 2000; vonHoldt *et al.* 2011; Rueness *et al.* 2011; Chambers *et al.* 2012).

Currently recognized as a single species, the red fox (*Vulpes vulpes*) has the widest natural distribution of any terrestrial carnivore, possibly any terrestrial mammal (Schipper *et al.* 2008). Its range spans approximately 70 million km^2, encompassing much of Europe, Asia and North America and extending into North Africa, with an introduced population in Australia (Larivière & Pasitschniak-Arts 1996; Macdonald & Reynolds 2004; Schipper *et al.* 2008). The red fox occupies a wide variety of ecosystems, including forests, grasslands, deserts and agricultural and human-dominated environments (Larivière & Pasitschniak-Arts 1996; Macdonald & Reynolds 2004). This fox also exhibits considerable phenotypic and life history variation at both large and small geographic scales (Lloyd 1980; Larivière & Pasitschniak-Arts 1996; Williams *et al.* 2004; Sacks *et al.* 2010). The fossil record indicates that red foxes evolved somewhere in Eurasia and colonized North America during or prior to the Illinoian (penultimate) glaciation (~300–130 kya; Kurtén 1968; Kurtén & Anderson 1980; Aubry 1983). Initially, the North American red fox was described as a distinct species (*Canis fulvus*, Desmarest 1820) and continued to be considered as such (*Vulpes fulva*) until the mid-20th century when Churcher (1959) recommended combining red fox taxa based on analysis of a single, somewhat arbitrary character (molar cusp patterns; Appendix S1, Supporting Information).

To date, genetic studies of red foxes have been based on insufficient genomic and geographic coverage to understand their global evolutionary history or to evaluate the taxonomic status of North American red foxes. Mitochondrial DNA (mtDNA) sequences from Europe, northern Asia and North America pointed to ancient intercontinental divergence in the mid-Pleistocene, followed by secondary contact during the middle of the last glaciation (Aubry *et al.* 2009). However, assessing

speciation depends in part on the extent of genomic transfer during this secondary contact, as well as the depth of intercontinental relative to intracontinental genomic divergence. Thus far, the only applications of nuclear DNA (nDNA) in population genetic studies of the red fox have been regionally restricted and limited to microsatellites and a small number of SNPs (e.g. Sacks *et al.* 2010, 2011; Statham *et al.* 2012a). Microsatellites provide little information on more ancient timescales because of their high mutation rates and size homoplasy, which mask phylogenetic signals; SNPs, while potentially useful, need to be developed from representative population samples, which is difficult to know a priori (Sacks & Louie 2008). No study has examined the Y-chromosome ancestry of red foxes, which would provide a male-specific phylogeographic understanding independent of that resulting from mtDNA.

The geographic coverage of previous genetic studies on the red fox has been incomplete. Although numerous studies have been conducted at regional scales (e.g. Frati *et al.* 1998; Inoue *et al.* 2007; Sacks *et al.* 2010, 2011; Statham *et al.* 2011, 2012b; Teacher *et al.* 2011; Edwards *et al.* 2012), only two have spanned continents (Aubry *et al.* 2009; Kutschera *et al.* 2013), and none has included southern portions of Asia and North Africa, where red foxes, similarly to many other mammals, are likely to have persisted during the Pleistocene glaciations (Hewitt 1999; Sharma *et al.* 2004; Marmi *et al.* 2006; Davison *et al.* 2011).

Here, we investigate the global phylogeography and species-level systematics of the red fox using a suite of matrilineal, patrilineal and biparentally inherited genetic markers from samples collected throughout its range, including regions unrepresented in previous phylogeographic studies. Our broad objectives were to assess the geographic origins of the red fox, compare historical demography on North American and Eurasian continents and characterize the temporal divergence between continental populations. We were especially interested in assessing the concordance of intercontinental relationships reflected by mitochondrial and nuclear markers and, in doing so, re-evaluating the genome-wide phylogenetics of red foxes.

Materials and methods

Samples

We used 1164 red fox samples collected throughout the species' range (Table S1, Supporting Information). We also included an Arctic fox (*Vulpes lagopus*), a kit fox (*Vulpes macrotis*) and a fennec fox (*Vulpes zerda*) as outgroups. Red fox samples included 450 DNA samples collected for this study, 714 samples from our previous studies (Perrine *et al.* 2007; Aubry *et al.* 2009; Sacks *et al.* 2010, 2011; Statham *et al.* 2011, 2012a,b; Edwards *et al.* 2012) and others in southern Europe and Japan (Frati *et al.* 1998; Inoue *et al.* 2007). We reamplified and resequenced mtDNA fragments from 76 red foxes used by Edwards *et al.* (2012) because that study used shorter mtDNA fragments than the present one. The 450 new samples included blood and tissue ($n = 183$), museum specimens (skin snips, nasal turbinate bones and bone chips, $n = 87$), hair ($n = 51$) and scat ($n = 129$). The museum specimens were from the Harrison Institute, Natural History Museum in London, Harvard Museum of Comparative Zoology, Yale Peabody Museum of Natural History and National Museum of Natural History, Washington, DC (Appendix I). We selected subsamples for nuclear marker analyses ($n = 85$ for Y-chromosome, $n = 51$ for autosomal) based on two criteria: broad geographic representation and high DNA sample quality and quantity (Table S1, Supporting Information). This sample set covered all major regions except North Africa, for which we did not have samples of sufficiently high DNA quantity to enable nuclear analyses.

Laboratory procedures

Extraction of DNA, PCR and sequencing methods for mtDNA were described in detail previously (Aubry *et al.* 2009; Statham *et al.* 2012b). Briefly, we extracted DNA from museum specimens in designated ancient DNA or natural-history DNA laboratories and used multiple DNA-extraction- and PCR-negative controls. We amplified two mtDNA regions, a 354-bp portion of the cytochrome *b* gene (primers RF14724 and RF15149, or for degraded samples RF14724 and RFCYTB3R, and RFCYTBBF and RF15149; Perrine *et al.* 2007) and a 343-bp portion (including insertions and deletions) of the D-loop (primers VVDL1 and VVDL6; Aubry *et al.* 2009). For degraded samples, we designed two internal D-loop primers (VVDL4: 5′-CGAGGCATGGTGATAAATCC - 3′ and VVDL5: 5′-TGACTGCACGTCACTTAGTCC-3′), which amplified smaller overlapping fragments of the D-loop region using primer pairs VVDL1/VVDL4 and VVDL5/VVDL6.

We used primers corresponding to ~4300 bp derived from the Y-chromosome in the domestic dog (Natanaelsson *et al.* 2006) to resequence red foxes in search of Y-chromosome microsatellite markers. Following the PCR protocol of Natanaelsson *et al.* (2006), we amplified putative Y-chromosome sequence of male red fox and identified two novel dinucleotide repeat microsatellite loci. We then designed primers to amplify these loci in shorter amplicons (Table S2, Supporting Information)

and combined the two loci into a single multiplex assay with the forward primers labelled with a 6-FAM fluorescent tag. We conducted PCR and genotyping using the same methods described for autosomal microsatellites (Sacks *et al.* 2011), except that annealing temperature was set at 60 °C. We attempted to amplify these loci in nine females along with four male controls. Only the males amplified confirming the Y-chromosome positioning of these markers in red foxes, as was expected given high homology among sex chromosomes of red foxes and dogs (Bugno-Poniewierska *et al.* 2012).

Lastly, we amplified and sequenced 11 autosomal DNA loci corresponding to anonymous canine BAC ends (Sacks & Louie 2008) totalling 2784 bp. We used previously published primers, PCR chemistry and cycling conditions (Sacks & Louie 2008; loci 11, 12, 17, 18, 20, 23, 35, 38, 41, 42, 48). We amplified all loci in small fragments (<350 bp) to maximize amplification success. To choose loci, avoid linkage and obtain a better representation of the red fox genome, we first determined the chromosome positioning of each locus in the dog genome using 'BLAST-Like Alignment Tool' (BLAT) on the University of California, Santa Cruz genome browser (Kent 2002). We then mapped these regions to the red fox genome by cross-referencing with a red fox linkage map (Kukekova *et al.* 2007). In the one instance where we determined that two gene regions were on the same red fox chromosome, they were located >15 centimorgans (cM) apart.

mtDNA data analysis

We conducted all mtDNA analyses on concatenated cytochrome *b* and D-loop sequences unless otherwise noted. We constructed Bayesian phylogenetic trees using MrBayes 3.1.2. (Ronquist & Huelsenbeck 2003). We assessed the most appropriate model of DNA substitution for each data set using the Akaike Information Criterion in jModelTest 0.1.1 (Posada 2008). For the combined cytochrome *b* and D-loop sequences, we partitioned the data set into four regions: 1st, 2nd and 3rd codon positions of the cytochrome *b* gene, and the D-loop. For the cytochrome *b* portion of the data set, we used a HKY model of DNA substitution and the gamma distribution shape (HKY+G); for the D-loop, we used GTR +I+G. We estimated branch lengths independently using RAxML (Stamatakis 2006) and used the resulting parameter as an input value in MrBayes. We used default values for other parameters. We then reran MrBayes for 12 000 000 generations, with two runs of four independent chains running simultaneously (with one heated), and sampled one tree every 1000 generations. We checked runs for convergence (i.e. average standard deviation of split frequencies approached 0.01, potential scale-reduction factor approached 1.0). Our analysis resulted in 24 000 sampled trees. We plotted the log-likelihood scores and determined that a 10% burn-in was appropriate because the values had reached an asymptote. We then constructed a phylogenetic tree and calculated Bayesian posterior probability (BPP) support values at the nodes based on the 21 600 remaining trees. Five independent runs produced trees of very similar topology.

We used ARLEQUIN 3.5 (Excoffier & Lischer 2010) to estimate haplotype and nucleotide diversity and to generate two neutrality statistics (Tajima's *D* and Fu's *Fs*) to detect signatures of past demographic events (Tajima 1989; Fu 1997). We created median-joining networks (Bandelt *et al.* 1999) in Network 4.6.1.0 (www.fluxus-engineering.com) with cytochrome *b* mutations conservatively weighted double that of the D-loop (Sacks *et al.* 2010). We used a fixed mutation rate to estimate divergence times, both within and among clades, by calculating the average number of mutations (rho) between ancestral and descendant haplotypes in mtDNA haplotype networks (Forster *et al.* 1996; Saillard *et al.* 2000). Mutation rates were estimated at 10.16% per million years in the concatenated 697-bp fragment, based on weighted averages estimated for D-loop and cytochrome *b* DNA (Aubry *et al.* 2009; Edwards *et al.* 2012). For comparison, and especially to safeguard against underestimation of the ages of the earlier branching points, we also calculated divergence-time estimates in BEAST 1.7.5 (Drummond & Rambaut 2007) using a combination of root and tip dating, although such estimates are prone to overestimation due to homoplasy (Appendix S2, Supporting Information).

We calculated the degree to which population genetic differences could be explained by isolation by distance using 1000 permutations of Mantel tests of geographic distances vs. pairwise Φ_{ST} in ARLEQUIN 3.5.1. We used a spatial analysis of molecular variance in SAMOVA 1.0 to identify phylogeographic discontinuities (Excoffier *et al.* 1992; Dupanloup *et al.* 2002). We ran the analysis for 100 simulated annealing processes, with the numbers of geographic groupings (*K*) ranging from 2 to 10. Analysing multiple levels of *K* enabled us to determine the most basal population subdivisions, as well as finer-scale differentiation.

We estimated the timing of the secondary transfer of mtDNA from Asia to North America (Aubry *et al.* 2009) and the likelihood of subsequent gene flow using Markov chain Monte Carlo (MCMC)-based simulations in the program IMa (Hey & Nielsen 2007). To minimize the effects of substructure in the mtDNA data set, we restricted our analyses to Holarctic haplotypes in East Asia (Eastern Russia, Mongolia, China; $n = 74$) and

Alaska (n = 51). Parameterization and search criteria are detailed in Appendix S3 (Supporting Information).

To detect whether demographic changes associated with glacial cycles were evident in the genetic diversity, we used the Bayesian skyline plot coalescent method in BEAST (Drummond *et al.* 2005). We analysed the cytochrome *b* portion of the mtDNA data set partitioned into codon positions 1 + 2, and 3 (as recommended by Shapiro *et al.* 2006), the HKY+G substitution model, 10 skyline groups and a strict molecular clock. We assumed a mutation rate of 2.8% per million years (see Aubry *et al.* 2009). For the North American data set, we ran 40 million generations, and for the larger Eurasian/African data set, we ran 100 million generations, both with a 10% burn-in. We ran multiple independent MCMC runs for each data set and used Logcombiner to combine the output from three separate runs with effective samples >200. We visualized results using Tracer.

Nuclear DNA data analysis

We grouped alleles from the two linked Y-chromosome microsatellite loci into haplotypes for each individual. We assessed topology among haplotypes using Network with loci weighted inversely to observed numbers of alleles (Sacks *et al.* 2013). Specifically, locus Y29 was given a weight of 8, while locus Y30 was given a weight of 7.

For autosomal loci, we used the Bayesian algorithm from the program Phase (implemented in DNAsp 5.1) to infer haplotypes from diploid sequences (Librado & Rozas 2009). Initially, we accepted assigned nucleotides with probabilities ≥75%. Six loci exhibited heterozygous sites that were unresolved at this probability cut-off. Consequently, we used the program Network to produce haplotype networks for tentatively phased haplotypes (with equal weight given to all substitutions). We used these networks to judge the effect of parsing alleles from the heterozygous sites with lower support. If one of the calls caused reticulation in the network, the alternative was checked; if the alternative avoided reticulation, it was adopted. Where the alternative base assignment also generated reticulation elsewhere, the nucleotide site was left unresolved. Following screening with IMgc (Woerner *et al.* 2007), loci with evidence of recombination were trimmed, as were haplotypes with unresolved sites.

We calculated the number of alleles (A), observed heterozygosity (H_o) and expected (under Hardy–Weinberg equilibrium) heterozygosity (H_E) in ARLEQUIN and private allelic richness in HP-Rare (Kalinowski 2005). We tested for deviations from Hardy–Weinberg equilibrium using ARLEQUIN and from gametic equilibrium using Genepop (http://genepop.curtin.edu.au/).

We examined global red fox substructure with the model-based Bayesian clustering method in Structure 2.3.3, specifically using the admixture model with correlated allele frequencies (Pritchard *et al.* 2000; Falush *et al.* 2003). We converted haplotypic DNA sequences into distinct alleles, phlyogenetically equidistant from one another (i.e. treated irrespectively of pairwise differences between haplotypes). Iterations were run from K = 1–7 for 500 000 generations, discarding the first 100 000 as burn-in. We ran simulations five times for each value of K. All iterations were run blind (i.e. without prior geographic information). This technique does not require that individuals are assigned to predefined populations, thus allowing for an objective assessment of population subdivision.

We were interested in determining the phylogenetic relationship and divergence time between Eurasian and North American red fox populations. To achieve this, we first created species trees using a Bayesian coalescent-based method in *BEAST 1.7.5 (Heled & Drummond 2010). This method assumes no gene flow after divergence, which we presume was not strictly the case, but violation of this assumption would result in underestimations of divergence times. The analysis used sequence data from multiple loci to simultaneously estimate multiple gene trees embedded in a shared species tree. We used the divergence-time estimates from Perini *et al.* (2010) for internal calibration on the following branching points: fennec fox vs. all other *Vulpes* (4.99, 3.68–6.48 myr); Arctic fox vs. kit fox (0.97, 0.55–1.45 myr) and Arctic and kit foxes vs. red fox (2.91, 2.09–3.84 myr). Uncertainty in the Perini *et al.*'s (2010) estimates was incorporated using a normal distribution prior around each time point. We used a Yule prior on the species tree (Drummond *et al.* 2007). We used a strict clock model of sequence evolution because the relaxed uncorrelated log-normal clock approach showed little rate heterogeneity among lineages. We used the most appropriate model of sequence evolution for each locus as determined by program jModelTest. We ran *BEAST for 800 000 000 generations, sampling every 80 000 generations, which resulted in 10 000 samples. A second run with the same settings yielded the same topology and very similar age estimates; therefore, the two were combined using Logcombiner (distributed with BEAST). Based on the analyses of the resulting data in Tracer 1.5 (Rambaut & Drummond 2007), we discarded the first 10% of trees as burn-in. All parameters of both runs had effective sample sizes (ESS) >100. The combined runs had ESS values >200 for most parameters, including all divergence-time estimates.

As a second means of estimating the divergence time between Eurasian and North American red foxes, while also allowing for the possibility of postcolonization

genetic exchange, we used MCMC-based simulations in IMa. We used a likelihood ratio test to choose among nested models with and without the possibility of gene flow (Hey & Nielsen 2007). In principle, this approach enabled the joint estimation of divergence time and gene flow (if any). Parameterization and search criteria are detailed in Appendix S3 (Supporting Information).

Results

Mitochondrial DNA

We obtained cytochrome *b* sequences for 1068 individuals and D-loop sequences for 959 individuals, resulting in 927 combined cytochrome *b* and D-loop sequences. We obtained 135 unique cytochrome *b* haplotypes, half (n = 67) of which were previously unreported, and 232 unique D-loop haplotypes, 70% (n = 163) of which were previously unreported (GenBank Accession nos KJ846508–KJ846756, KG959959–KG960060, KM263585–KM263587). Altogether, we identified 285 distinct combined cytochrome *b* and D-loop mtDNA haplotypes from red foxes.

The Bayesian phylogenetic tree of mtDNA haplotypes grouped red foxes together with high support (Fig. 1) and to the exclusion of other *Vulpes* species. We identified two well-supported (BPP 0.97–1.0) reciprocally monophyletic clades that were geographically distinct, corresponding to the previously named 'Holarctic' and 'Nearctic' clades, as well as a third clade with lower support (BPP 0.79) restricted to Africa that was reciprocally monophyletic with respect to the combined Holarctic and Nearctic clades. The Holarctic clade contained the greatest number of haplotypes and individuals and was also the most widely distributed, occurring in North Africa, the Middle East, Europe, Asia and North America. Haplotypes that were basal to the three nested clades were found only in the Palaearctic, in Africa and in more southern areas of Asia, especially the Middle East (Fig. 2). There were no shared haplotypes between North America and other continents.

Using Rho statistics, we estimated the time to most recent common ancestor (TMRCA) of the clade containing all red foxes at 1.15 (0.85–1.45) million years ago and the three nested clades at 88–102 kya (Fig. S1, Table S3, Supporting Information). We estimated the TMRCA of the combined Nearctic clade and Holarctic clade at 399 (260–538) kya. Analyses run in BEAST with age calibration based on divergence times of the out-group fox species generated considerably earlier estimates, regardless of whether or not tip dating was included (Fig. S1, Supporting Information), much more so than supported by the fossil record (e.g. Kurtén & Anderson 1980). For

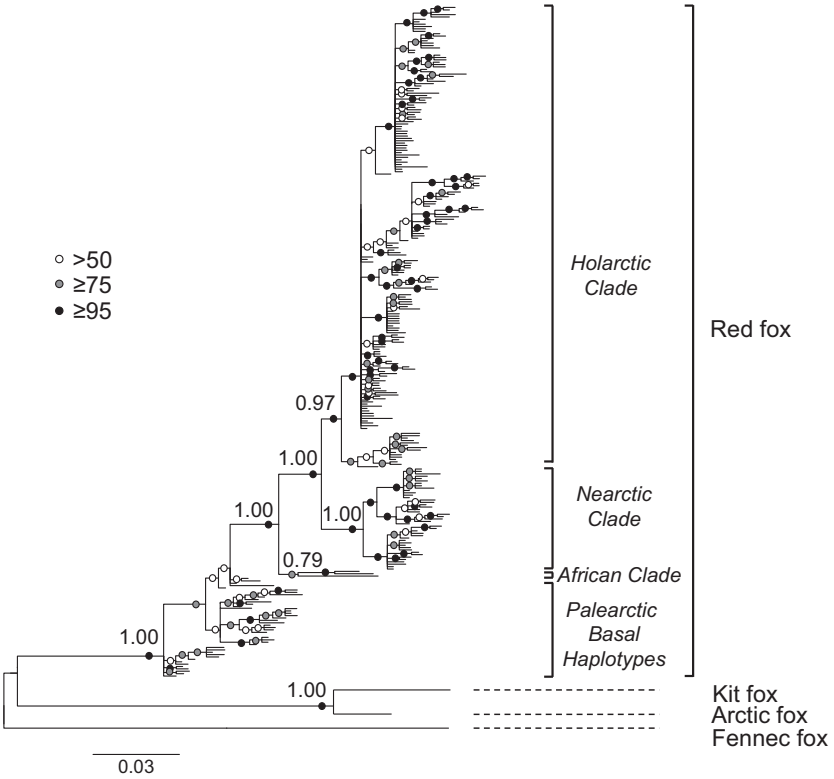

Fig. 1 Phylogenetic tree of global red fox mitochondrial DNA created in MrBayes from 698 bp of concatenated cytochrome *b* and D-loop sequences comprising 285 distinct haplotypes from 901 red foxes and three from out-group fox species. Bayesian support values are indicated at the nodes with shaded circles, and, for selected nodes, numerical values. The scale bar units are nucleotide substitutions per site.

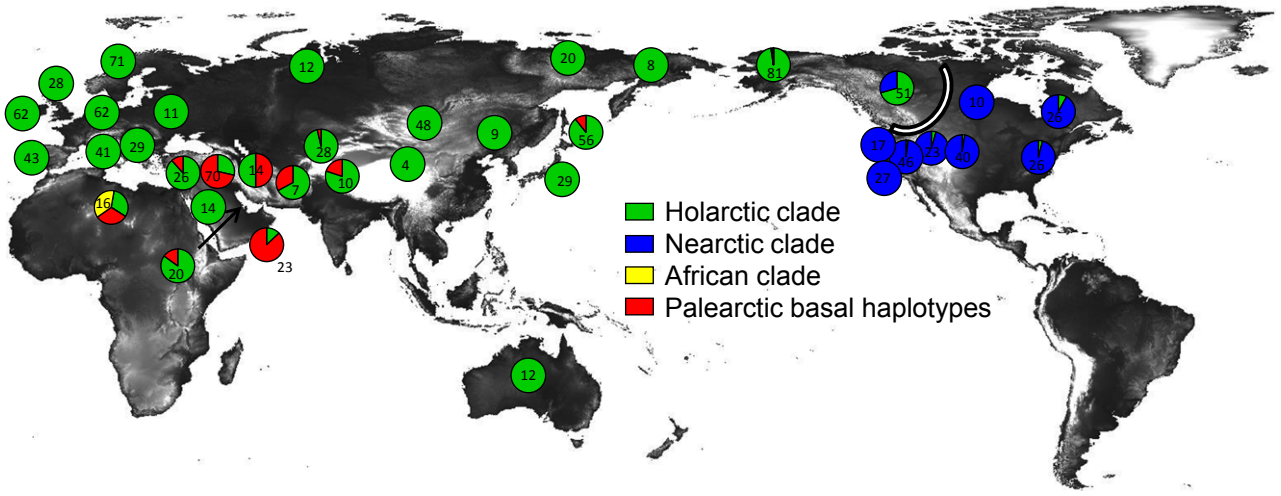

Fig. 2 Geographic distribution of red fox sampling sites, samples sizes and mitochondrial clades. Each pie chart represents the phylogenetic make-up of individuals sampled in that area. The clades correspond to those identified in Fig. 1. The most basal phylogeographic break (K = 2) identified by SAMOVA is indicated with a black and white line. We included all individuals (n = 1109) that could successfully be assigned to a clade, including individuals with partial sequences (either cytochrome *b* or D-loop).

example, the TMRCA of the clade containing all red foxes was estimated at 4.04 (3.21–4.49) mya, which overlapped the 2.91 (2.09–3.84) mya calibration point for the TMRCA of red foxes with kit and Arctic foxes. The major clades for the red fox were estimated at 2.57–3.16 mya, which also overlapped this calibration point. As these results were considerably older than the current interpretation of the fossil record (e.g. Kurtén & Anderson 1980) and inconsistent with various vicariant explanations (Aubry *et al.* 2009; Sacks *et al.* 2010; Edwards *et al.* 2012), we limited our interpretations to those based on rho-derived mtDNA divergence-time estimates.

The SAMOVA analysis resulted in statistically significant Φ_{CT} values at K = 2–10. The most fundamental division (K = 2, Φ_{CT} = 0.436) reflected the geographic distribution of Nearctic clade haplotypes vs. all others (Fig. 2). As noted previously (Aubry *et al.* 2009), although the Holarctic clade occurred on multiple continents, all North American representatives of this clade belonged to the endemic Alaskan subclade (H III; Figs S2, S3, Supporting Information).

Estimates for the mtDNA splitting time between adjacent populations in Alaska and East Asia pre-dated the end of the last glacial period and provided no evidence of subsequent gene flow (Table 1). Specifically, both the 'isolation-only' and 'isolation-with-migration' models indicated similar matriline splitting times of ~40–43 kya (combined 90% HPD: 21–64 kya), and modal estimates of gene flow (in the 'isolation-with-migration' model) approached zero in both directions. Analyses of the full Eurasia/Africa vs. North America data set suggested a similar if slightly earlier splitting time of 49 kya (90% HPD 32–66) along with estimates of gene flow abutting zero (Table S4, Supporting Information). Together, these analyses suggest that the secondary transfer of the (currently) Holarctic haplotype was a one-time event, rather than reflective of constant or repeated gene flow.

The mtDNA of North America and Eurasia/Africa showed strikingly different historical demographic

Table 1 Mitochondrial DNA splitting time and demographic analyses of red fox populations on either side of the Bering Strait in Alaska and East Asia. Analyses based on 697 bp of concatenated cytochrome *b* and D-loop sequences. IMa jointly estimates the demographic parameters of N_e ($\theta/4\mu$), N_em ($\theta m/4$) and population splitting times (t/μ). The 90% highest posterior density (HPD) intervals are given in parentheses after each of the parameter estimates

Demographic Model	N_e Alaska (×1000)	N_e East Asia (×1000)	N_e Ancestral (×1000)	N_em into Alaska (per 1000 years)	N_em into East Asia (per 1000 years)	Splitting time (×1000 years)
Isolation only	119 (65, 172)	227 (169, 360)	91 (7, 172)	–	–	40 (24, 55)
Isolation with migration	110 (57, 163)	261 (163, 355)	97 (4, 187)	0.001 (0, 0.003)	0.0006 (0, 0.0012)	43 (21, 64)

patterns. The Bayesian skyline plot of North American red foxes indicated an increase in population size following the retreat of Wisconsin glaciers (~12 kya, Fig. 3). The Eurasian/African red fox populations displayed a signature of expansion starting approximately 50 kya during the last glacial period (Würm/Wisconsin) that began to plateau prior to the last glacial maximum (26–19 kya). The expansion indicated in Fig. 3 primarily reflected the Holarctic clade, which produced a very similar skyline plot when analysed on its own (data not shown). The Holarctic clade is distinguished by relatively few missing haplotypes and shorter branch lengths between nodes, consistent with population expansion or positive selection. A selective sweep or population expansion affecting the Holarctic clade was also supported by significantly negative Tajima's D (-1.522, $P = 0.024$) and Fu's F_S statistics (-23.89, $P = 0.002$). Neutrality tests for the Nearctic clade were generally consistent with an expansion as well, but were weaker, including a nonsignificant negative Tajima's D (-0.668, $P = 0.299$) and a significant Fu's F_S statistics (-11.73, $P = 0.012$).

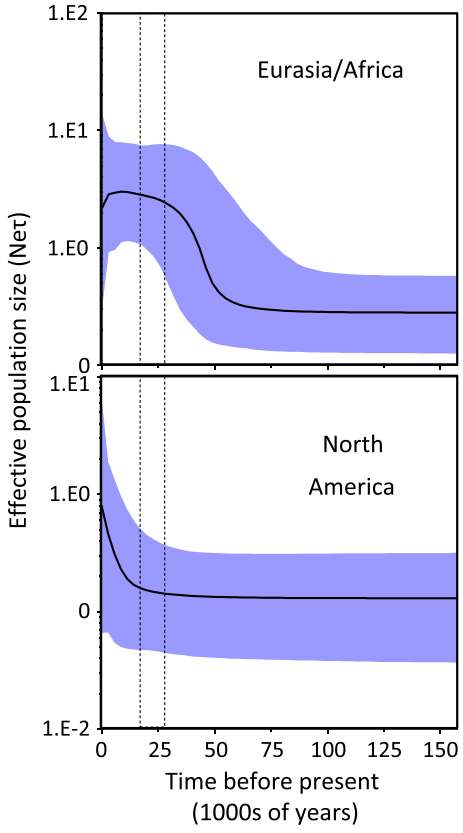

Fig. 3 Bayesian skyline plots derived from 354 bp of the cytochrome b gene for Eurasian/African ($n = 674$), and North American ($n = 288$) specimens. The x-axis represents time in units of 1000 years. The y-axis represents effective population size as $N_e\tau$ on a log scale. The black line depicts the median population size, and shaded areas represent the 95% highest posterior density. The time period around the last glacial maximum is indicated by the dashed line.

Nuclear DNA

Based on 85 male specimens representing most of the red fox's global range, we identified sixteen Y-chromosome haplotypes, five in North America and 11 in Eurasia. In contrast to mitochondrial DNA, Y-chromosome haplotypes mapped to mutually exclusive continent-specific clades: one in North America and two in Eurasia (Fig. 4). The Y-chromosome data set included North American individuals bearing Holarctic and Nearctic clade mtDNA haplotypes in similar proportion to their representation in the mtDNA data set (Table S1, Supporting Information; Dryad). We created a second network without any weighting to assess the robustness of the network to the particular weighting scheme. The unweighted network resolved the same three continent-specific clades, but introduced a reticulation within clade 1. Similarly to mtDNA, North American Y-chromosome haplotypes were more closely related to one another than Eurasian haplotypes, consistent with a younger, smaller North American lineage. Within Eurasia, clade 1 contained individuals from throughout Europe and the Middle East, while clade 2 contained individuals from Asia (outside the Middle East) and northern Europe.

After phasing diploid autosomal sequences (147–325 bp each), IMgc identified and trimmed four loci

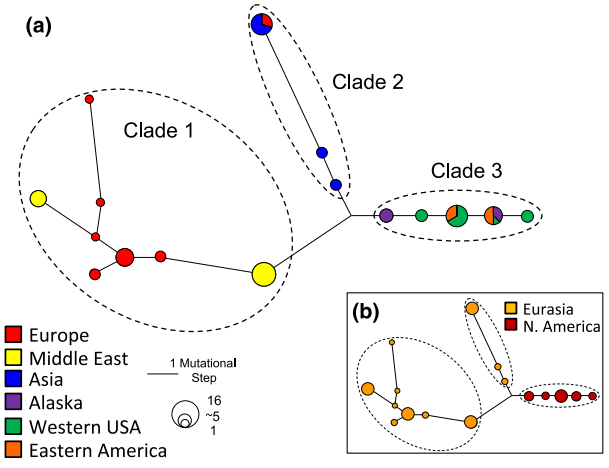

Fig. 4 Haplotype network of red fox Y-chromosome haplotypes of 85 male red foxes. Branch lengths are proportional to the number of stepwise mutations, and circle sizes are proportional to the number of individuals represented. Part (a) displays the geographic regions considered, while part (b) is colour coded by continent.

with potential recombination, reducing the data set from 2784 to 2701 bp. From these data, we identified 90 distinct haplotypes across 11 loci, for an average of 8.2 haplotypes per locus among the 108 autosomes (1188 gene copies; Fig. S4, Supporting Information). Tests for gametic disequilibrium identified three population locus-pairs that were statistically correlated (North America: Loci 11, 38; Loci 12, 41; Eurasia: Loci 18, 20). Seven loci were identified with significant deviations from Hardy–Weinberg equilibrium (North America: Locus 12, 17, 35, 38, 42; Eurasia: Locus 17, 42), none of which was out of equilibrium when intracontinental regions were analysed. In general, deviations from linkage and Hardy–Weinberg equilibria were inconsistent across loci and locus-pairs, and more in line with substructure than null alleles or physical linkage. Therefore, we retained all loci in subsequent analyses.

Bayesian cluster analysis of 11 nuclear loci in program Structure indicated that $K = 2$ corresponded to the highest posterior probability across all five iterations of $K = 1$–7. In contrast to expectations based on the mtDNA, the nDNA analysis at $K = 2$ partitioned global red fox populations into distinct North American and Eurasian clusters, without a priori geographic information (Fig. 5). As with the Y-chromosome data set, the autosomal data set included North American individuals bearing Holarctic and Nearctic clade mtDNA haplotypes in approximate proportion to their representation in the mtDNA data set (Table S1, Supporting Information; Dryad). Higher K values resulted in sharply decreasing log probabilities of the data and in uninformative and nonsensical clusters partitioning individuals within continents equally among the additional groups. Analyses of each of the individual continental clusters separately indicated that $K = 1$ had the highest support, with uninformative clusters being produced at higher values of K.

Phylogenetic analysis using the 11 nuclear gene regions resulted in a well-supported tree, with Eurasian and North American red foxes grouping as sister taxa (Fig. 6). Conservatively assuming no intercontinental gene flow since colonization, we estimated that North American and Eurasian red fox populations split 209 kya (95% HPD 103–377 kya). If gene flow between continental populations had occurred since the initial colonization of North America (as indicated by the mtDNA), this estimate would tend to underestimate the time since colonization. Additional phylogenetic analyses in *BEAST considering the six continental regions as tips also resolved continent-specific lineages (data not shown). Similarly, pairwise F_{ST} values indicated a closer relationship between regions within continents (0.03–0.10) than between continents (0.19–0.37; Table S5, Supporting Information). Eurasian and North American continental populations differed significantly (F_{ST} = 0.23, $P < 0.0001$). Autosomal genetic diversity was higher in Eurasian than in North American red foxes, consistent with mtDNA and Y-chromosome markers (Table 2).

Analyses of the autosomal data set with the 'isolation-only' model in IMa indicated a splitting time between continental lineages of 165 kya (90% HPD: 71–257 kya; Table 3), similar to that estimated from the phylogenetic analysis of these data above, but considerably earlier than the mtDNA splitting time estimates (Fig. 7). The likelihood ratio test rejected all five possible 'isolation-only' models ($P < 1.3 \times 10^{-99}$), suggesting that some gene flow occurred since initial divergence

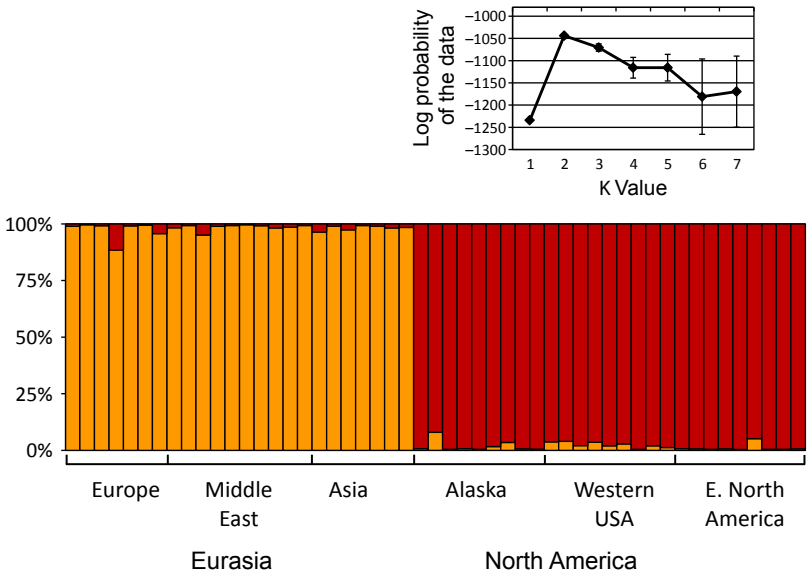

Fig. 5 Bayesian cluster analysis of individual red foxes generated in the program Structure. The output is generated based on the allelic make-up of 51 red foxes at 11 nuclear sequence loci. Vertical bars represent individual foxes, and the shading represents the proportional assignment to different clusters. The inset graph displays the support value for each level of K. $K = 2$ consistently had the highest support across five iterations of $K = 1$–7.

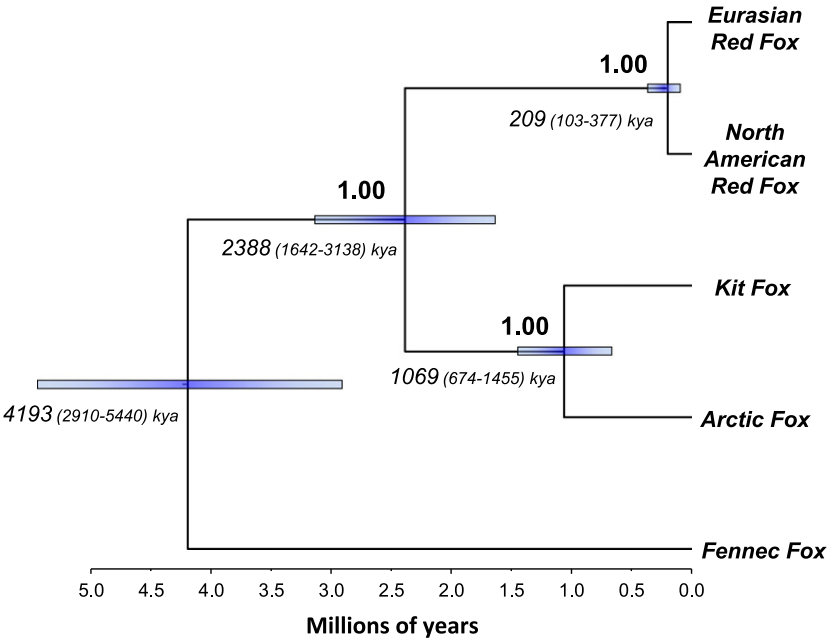

Fig. 6 Phylogenetic tree and divergence-time estimates for Eurasian and North American red foxes. The tree and time estimates were created in the program *BEAST based on sequences from 11 independent nuclear loci from 48 (2n) Eurasian and 54 (2n) North American red foxes. Numbers at the nodes in bold indicate Bayesian posterior probabilities, with those in italics indicating divergence-time estimates in thousands of years (kya) and those in parentheses indicating the 95% highest posterior density values around each age estimate (also indicated by bars surrounding each node).

(i.e. consistent with mtDNA). When considering the 'isolation-with-migration' models, all posterior estimates of migration in both directions approached zero, yet resulted in far older splitting time estimates (90% HPD = 0.5–8.9 mya; Table 3). The gap between the upper HPD of the 'isolation-only' model and the lower HPD of the 'isolation-with-migration' model probably reflected a poor fit of the IMa model options, which assume either no migration at all after splitting (isolation-only model) or continuous migration since splitting (isolation-with-migration model). Gene flow between continents would only have been possible during periods of lower sea level (i.e. glaciations). Thus, our findings suggest that divergence was indeed followed by some gene flow and that splitting began prior to the time estimated by the isolation-only model.

Table 2 Nuclear genetic variability of Eurasian and North American red foxes based on 11 nuclear loci in 51 red foxes, including the number of alleles (*A*), allelic richness (Ar), private allelic richness (PAr), observed heterozygosity (H_o) and expected heterozygosity (H_E)

Population	*n*	*A*	Ar	PAr	H_o	H_E
Eurasia	24	5.7	5.7	3.19	0.50	0.55
North America	27	3.5	3.4	0.86	0.26	0.37
Europe	7	4.2	3.8	0.73	0.52	0.64
Middle East	10	4.4	3.4	0.56	0.59	0.61
Asia	7	4.1	3.1	0.36	0.65	0.62
Alaska	9	3.0	2.4	0.11	0.35	0.42
Western USA	9	3.2	2.6	0.18	0.33	0.46
Eastern North America	9	2.7	2.2	0.15	0.30	0.41

Intracontinental mitochondrial subdivisions

Partitioning of mtDNA lineages into subclades in haplotype networks further elucidated intracontinental patterns (Fig. 8), revealing both geographically restricted

Table 3 Nuclear DNA splitting time and demographic analyses of red fox populations on either side of the Bering Strait. Analyses based on 2701 bp across eleven nuclear sequence loci. The 90% highest posterior density (HPD) intervals are given in parentheses after each of the parameter estimates. Although the migration rates abutted zero, likelihood ratio tests rejected all five possible models that did not allow migration ($P < 1.3 \times 10^{-99}$). Only the 'isolation-only' and 'isolation-with-migration' models allowing different population sizes are shown here

Demographic Model	N_e North America (×1000)	N_e Eurasia (×1000)	N_e Ancestral (×1000)	N_em into North America (per 1000 years)	N_em into Eurasia (per 1000 years)	Splitting time (×1000 years)
Isolation only	241 (100, 376)	2555 (629, 4710)	996 (645, 1344)	–	–	165 (71, 257)
Isolation with migration	252 (99, 392)	1169 (67, 1636)	626 (1, 1659)	0.001 (0, 0.002)	0.001 (0, 0.002)	3309 (486, 8913)

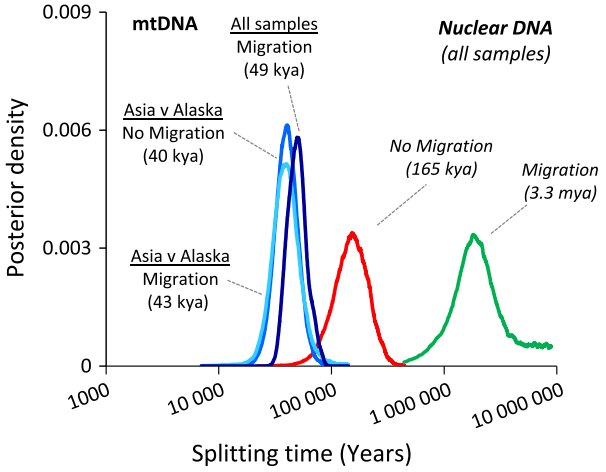

Fig. 7 Estimated splitting times between red fox populations either side of the Bering Strait. Estimates were generated in the program IMa. Mean values for each splitting time estimate are indicated. Models based on mtDNA yielded similar estimates regardless of whether they used all samples or only ones from Alaska and Asia, or incorporating migration or not. Models based on 11 nuclear sequences yielded generally older estimates.

and widely distributed lineages. Subclades indicated in the network were supported by ≥0.75 BPP in the phylogenetic tree (Fig. S2, Supporting Information), except for one network subclade (H III), which divided into several subclades in the tree (Fig. S3, Supporting Information). The Palaearctic basal haplotypes corresponded to four network subclades that were geographically restricted to Africa, the Middle East or East Asia. The Palaearctic subclade I, geographically restricted to the eastern corner of the Arabian Peninsula, was the most basal lineage within red foxes and thus may have had an important evolutionary position in the separation from other *Vulpes*. The Nearctic clade contained the three previously described subclades (Aubry *et al.* 2009). The Holarctic clade contained nine distinct subclades or tip clades, eight of which were found in Eurasia/North Africa, and one, subclade H III, which occurred strictly in North America, primarily near the Bering Strait in Alaska and Western Canada (Fig. 8). We found only two haplotypes in Australian foxes, both belonging to the same subclade as most British and Irish red foxes (Holarctic subclade IX, Fig. S3, Supporting Information). The most prevalent haplotype in Australia, U8-95, also occurred in England and the Netherlands, whereas the other haplotype, U8-96, only occurred in one sample from Ireland (for further description of all subclades, see Appendix S4, Supporting Information).

The SAMOVA also indicated subdivisions within continents, supporting previous findings (Aubry *et al.* 2009) and indicating new ones (Fig. 8). Support values (Φ_{CT}) plateaued from $K = 5$–7 and subsequently dropped. At $K = 7$ ($\Phi_{CT} = 0.486$), the following geographic groupings were identified: (1) Sierra Nevada, Rocky Mountains, Cascade Range, Great Basin, Sacramento Valley, USA; (2) Central Canada, Eastern Canada, Eastern USA; (3) Iran, Pakistan; (4) Eastern Arabia; (5) North Africa; (6) Honshu, Japan; and (7) all other populations. This subdivision was consistent with the population tree based on Φ_{ST} values (Fig. S5, Supporting Information). Within continents, we found a stronger relationship between Φ_{ST} and geographic distance in North America ($r^2 = 0.26$, $n = 10$, $P < 0.0001$) than in Eurasia and Africa ($r^2 = 0.05$, $n = 26$, $P = 0.028$).

Discussion

Our study of a worldwide sample of red foxes and a multimarker data set clarified past ambiguities resulting from use of a single genealogical marker and incomplete geographic sampling. A previous mitochondrial study using portions of the cytochrome *b* and D-loop loci (696 bp) suggested that long after North American red foxes originated from founders from Asia in the middle Pleistocene, they experienced a second wave of colonization during the last glaciation (Aubry *et al.* 2009). This conclusion was further supported by a subsequent analysis by Kutschera *et al.* (2013) of 335 bp of the D-loop from the same data set combined with additional data sets (e.g. Edwards *et al.* 2012) and by the present study, which added 450 samples from previously unsampled Middle Eastern, southern Asian and African portions of the range. Thus, it is well established that the maternal ancestry of North American red foxes was derived significantly from two distinct continental interchanges: an initial colonization during or prior to the Illinoian glaciation and a secondary infusion during the Wisconsin glaciation.

In contrast, our analyses of nuclear DNA indicated that the genomic ancestry of contemporary North American red foxes traced overwhelmingly to the initial colonization from Asia during or prior to the Illinoian glaciation, with very little genomic ancestry derived from the secondary contact episode that transferred the Holarctic mtDNA lineage (H III) during the last glaciation. Although our IMa analysis of autosomal sequences led us to reject a strict 'isolation-only' model (consistent with some degree of intercontinental nuclear genetic exchange), the posterior estimates of migration in the 'isolation-with-migration' model were minimal and included zero, indicating that the magnitude of nuclear genetic exchange must have been very low.

Moreover, if we assumed zero nuclear genetic exchange since initial colonization, estimates of the

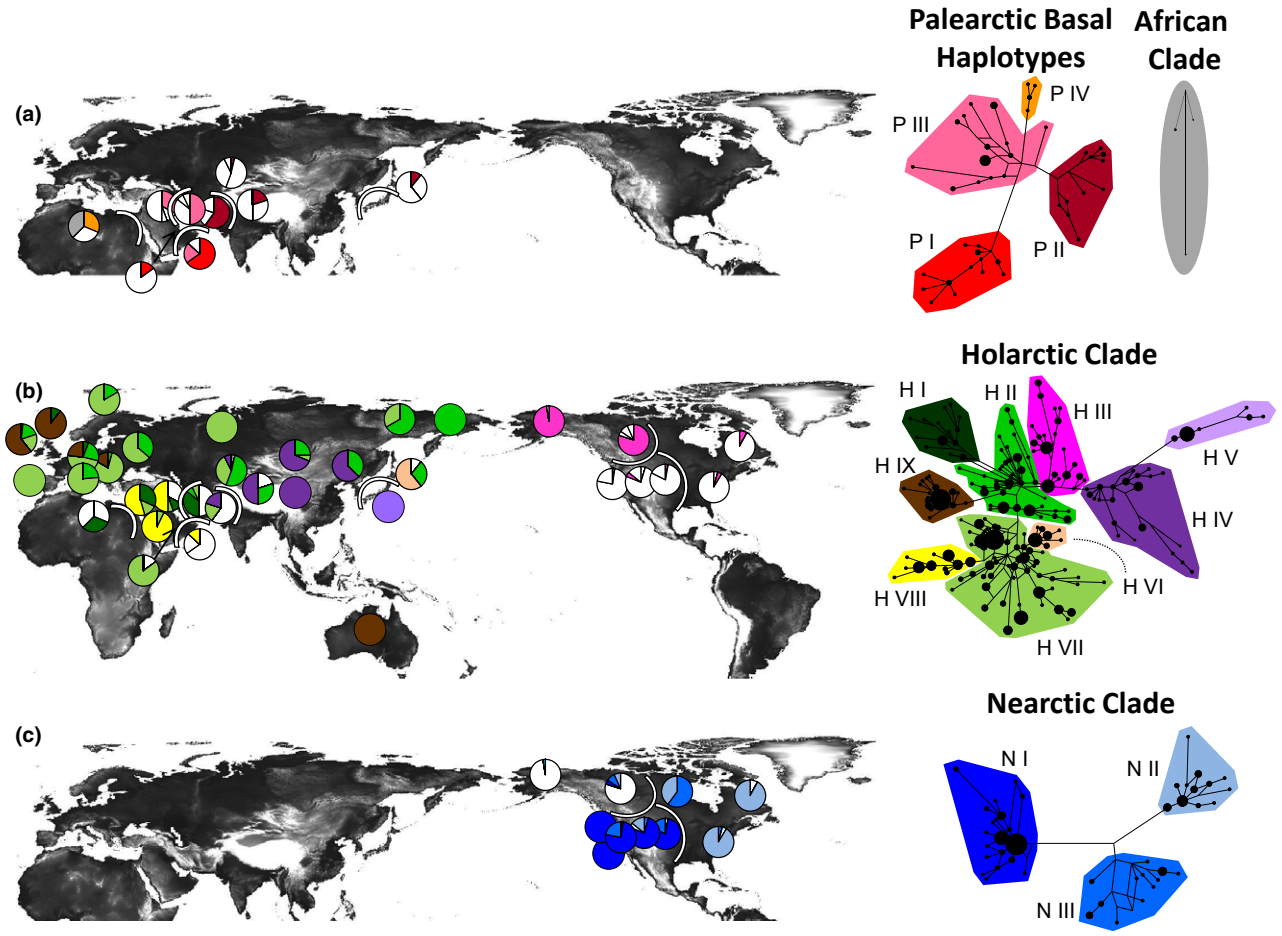

Fig. 8 Geographic distribution of red fox mitochondrial DNA clades and subclades. Subclade designations were based on concatenated cytochrome *b* and D-loop sequences, with the addition of single-gene sequences where the haplotype had sufficient resolution. Phylogeographic breaks identified by SAMOVA at $K = 7$ are indicated with black and white lines. The figure is split into three sections to allow easier visualization: (a) Palaearctic basal haplotypes and the African clade, (b) Holarctic clade and (c) Nearctic clade. The white sections of the pie charts indicate the portion of haplotypes belonging to a separate clade.

timing of this event (i.e. splitting time) from nuclear data were only slightly more recent than estimates of the TMRCA of the Nearctic and Holarctic mtDNA clades. In particular, both the 'isolation-only' model and Bayesian tree estimated that splitting times were consistent with the Illinoian glaciation, whereas the divergence time between the Nearctic and Holarctic mtDNA clades was estimated as slightly before the Illinoian glaciation ~400 kya (260–538 kya). Attempts to accommodate a small amount of genomic exchange in the estimate of splitting time did not work well, presumably due to forcing a one-time genomic transfer to be modelled as continuous gene flow (a constraint of the IMa program). The splitting time estimates covered a huge range, with highest posterior density spanning 0.5 to 9 mya. The higher end of this range was far earlier than supported by the fossil evidence (at least based on current interpretations), although the upper end of this range, ~0.5 mya, was in line with expectations from both the fossil record and mtDNA. The Y-chromosome haplotypes, which formed endemic continental clades, provided qualitative support for a deep continental division, although the two linked microsatellite loci provided insufficient genetic information to estimate temporal divergence. Analysis of a greater portion of the genome (e.g. via next-generation sequencing) will be necessary to quantify estimates of divergence times and the degree of nuclear genetic exchange more precisely, but the qualitative discordance between maternal and genome-wide patterns of phylogeography seems clear.

Such discordance, while not the norm, is also not unusual. In a recent review, nearly all (97%) similar incidences of mitochondrial/nuclear genetic discordance were attributed to secondary contact following long-term geographic isolation (Toews & Brelsford 2012). In allopatry and over time, mutations and

reproductive isolating mechanisms develop, which reduce, but do not completely prevent, interbreeding. Thus, the nuclear genome tends to reflect very low overall exchange, but due either to chance or to positive selection, the matriline can expand through a population even if based on a single interbreeding event. The discordance in this study between the apparent magnitude of mitochondrial and nuclear intercontinental exchange combined with the contemporaneous mtDNA expansion across Eurasia suggests the possibility that an advantageous mitochondrial mutation selectively swept across the northern portions of both continents prior to the last glacial maximum. Regardless of the cause of the mitochondrial introgression, the clear and deep continental division between the nuclear genomes of Eurasian and North American red foxes has significant implications for our understanding of speciation in this widespread taxon.

Intercontinental divergence and speciation

The taxonomy of red foxes has undergone several revisions, most of which did not include phylogenetic criteria. Historically, North American and Eurasian/African red foxes were considered to be distinct species based on morphological differences (Appendix S1, Supporting Information). In the mid-1900s, however, variation within a single character (cusp patterns on the first upper molar) was used as the basis for merging all red foxes into a single species, *Vulpes vulpes* (Churcher 1959; Appendix S1, Supporting Information). Our study provided an opportunity to reassess earlier taxonomic decisions based on robust phylogenetic and biogeographic evidence.

The fossil evidence further enabled us to place our findings into a more reliable chronological context. The earliest red fox remains from Eurasia date to >400 kya (Kurtén 1968). The earliest putative red fox specimen from Alaska dates to the Illinoian glaciation (~300–130 kya), and the earliest confirmed specimens in North America date to the Sangamon interglacial (~130–75 kya), indicating colonization across the Bering land bridge during or prior to the Illinoian glaciation (Péwé & Hopkins 1967; Kurtén & Anderson 1980; Aubry 1983; Pinsof *et al.* 1996). Until the continental glaciers receded, the initial colonists were restricted to ice-free refugia in northwestern North America. In the subsequent interglacial period, they would have been able to expand their range and colonize southern North America, as is evident from Sangamon fossil remains found in Idaho and Texas (Pinsof *et al.* 1996). Thus, taken together, the fossil record and genetic data indicate that red foxes colonized North America early in their history and have remained largely distinct through subsequent glacial/interglacial cycles.

The manner of divergence of North American red foxes from their Eurasian counterparts conforms well to the process of peripatric speciation, which occurs when a small, peripheral founder population receives a subset of the genetic diversity of the parent species (Mayr 1954). In isolation, this population undergoes an extended bottleneck with concomitant loss of diversity and changes in allele frequencies, which leads the species on an independent evolutionary trajectory from a very different genomic starting point. Whether such divergence among red foxes demonstrates speciation must be evaluated on the basis of multiple criteria, including comparative biogeography and systematics, postzygotic reproductive barriers and careful consideration of both ecological and adaptive contexts.

Two broad colonization patterns are evident among other Holarctic carnivore species (i.e. those with ranges spanning Eurasia and North America), such as the wolverine (*Gulo gulo*), grey wolf, brown bear (*Ursus arctos*) and Arctic fox. Either they colonized (or recolonized) North America during the Wisconsin glaciation (~75–11 kya; Kurtén 1968; Weckworth *et al.* 2010; Davison *et al.* 2011; McKelvey *et al.* 2014) or they remained connected continuously by sea ice (Norén *et al.* 2011). In contrast, carnivore genera that include sister species restricted to the Palaearctic and Nearctic (e.g. Eurasian [*Lynx lynx*] and Canadian [*L. canadensis*] lynx, sable [*Martes zibellina*] and American marten [*Martes americana*], steppe polecat [*Mustela eversmanni*] and black-footed ferret [*Mustela nigripes*]) have an older splitting time or earlier appearance in North America, dating back ~1 mya (Kurtén 1968; Johnson *et al.* 2004; Hughes 2012). The biogeographic history of the red fox as described in the present study represents a pattern that is intermediate between the two. Therefore, it may also be informative to consider intracontinental speciation during the Pleistocene as well. In North America, several carnivores that were isolated in disjunct refugia evolved into morphologically and genetically distinct species over time frames that ranged from <1 mya (American marten vs. Pacific marten [*M. caurina*]; Dawson & Cook 2012) to ~500 kya (e.g. swift fox [*V. velox*] vs. kit fox; Mercure *et al.* 1993). Thus, the splitting time of American and Eurasian red foxes is consistent with the time frames separating these North American sister species, including other *Vulpes* species.

Despite putative intercontinental translocations and more than a century of red fox fur-farming, there is surprisingly little information available on the reproductive compatibility of North American and Eurasian red foxes in captivity or, more importantly, in the wild (Statham *et al.* 2012b). However, based on our findings and other published mtDNA haplotypes from red foxes on both continents, it appears that the two continental

populations have remained largely distinct. For example, our mtDNA analysis of over 1000 individuals (and Y-chromosome analysis of 85 individuals) and many more from the literature failed to reveal a single cross-continental haplotype, suggesting that any recent historical cross-continental translocations must have at most a geographically limited legacy. The contemporary isolation of the two continents prevents genetic connectivity regardless of physiological or behavioural isolating mechanisms. Thus, taken together, our findings support the original two-species taxonomy for the red foxes of Eurasia/Africa (*V. vulpes*) and North America (*V. fulva*).

Intracontinental phylogeographic patterns and historical demography of red fox mtDNA

The estimated ages of mtDNA clades and subclades in North America and Eurasia were consistent with their origins during a time of intracontinental connectivity during the last interglacial period (Eemian/Sangamon), followed by allopatric fragmentation within continents during the last glacial period (Würm/Wisconsin). Demographic analyses suggested that after the last glacial maximum (26–19 kya), North American populations greatly expanded in size and geographic extent as the glaciers receded and large portions of the continent were revegetated (Fig. 3). In contrast, analyses of Eurasian/African populations indicated a marked increase in population size starting approximately 50 kya, with substantially slower growth before and after the last glacial maximum. Teacher *et al.* (2011) detected this relative stability from about 35 kya onwards in their analysis of European red foxes, but their skyline plot did not extend back beyond this time point and did not reveal the earlier expansion evident in our more extensive sample. The expansion seen in the full Eurasian/African data set reflects the history of the widespread Holarctic clade, which when examined on its own produced a similar skyline plot, while the basal and more centrally distributed Palaearctic lineages indicated a very gradual increase over time (M. J. Statham, unpublished data). The timing of this Eurasian population expansion coincided with the introduction of the Holarctic clade to North America and with the warmest period of the marine isotope stage 3 (MIS 3), which led to a reduction in steppe-tundra and an increase in tree cover in Beringia (Anderson & Lozhkin 2001).

Within North America, the four distinct mtDNA subclades (one Holarctic and three Nearctic) identified in the previous studies (Aubry *et al.* 2009; Sacks *et al.* 2010) were corroborated here. Within Eurasia and North Africa, divergent lineages were located primarily in southern regions. Red fox populations in northern portions of their range were less differentiated from each other (Fig. 8) and generally contained a subset of the total genetic diversity (Table S6, Supporting Information). This pattern was broadly consistent with the model of 'southern richness and northern purity' described for Northern Hemisphere taxa (Hewitt 1999). The most basal mtDNA lineages primarily occurred in the Middle East, suggesting that the red fox could have arisen in that region.

The occurrence of the most basal Eurasian/African phylogeographic breaks in the Middle East and North Africa was not surprising given their southern location and topographic variability, and the fact that the most ancient lineages of wolves (*Canis* spp.) have been identified in the same region (Sharma *et al.* 2004; Rueness *et al.* 2011). Multiple red fox subspecies have been described from North Africa, the Middle East and South Asia (Harrison & Bates 1991; Macdonald & Reynolds 2004). The geographic ranges for many of these subspecies have not been well defined, and their taxonomic validity has not been tested. However, there was a considerable overlap between the four described subspecies (*V. v. arabica*, *V. v. palaestina*, *V. v. flavescens* and *V. v. pusilla*) and the genetically differentiated populations revealed by our analyses (Appendix S5, Supplemental Information). Regardless of systematics, our mitochondrial findings put the extensive body of ecological and behavioural research on Eurasian red foxes into perspective. Specifically, most of these studies have been conducted in the northern portion of the range, which our findings suggest could reflect a single, relatively new, and minor segment of the phylogenetic diversity of this species in Eurasia and Africa. Thus, it is likely that future studies on southern Eurasian and African populations will reveal a broader and more representative understanding of the ecology and evolution of this highly successful generalist taxon.

Conclusions

Our study was one of the most comprehensive ever to investigate the phylogeographic consequences of Pleistocene climatic fluctuations on multiple continents. The mode of peripatric speciation we propose to describe the evolution of the North American red fox may provide a model for speciation in temperate sister species that are restricted either side of the Bering Strait. In such species, the progenitor probably originated in a more southern region of one continent, yet due to periodic northern linkages between the continents in Beringia, the daughter species originated in the northern portion of the secondary continent. Such a pattern seems predisposed to facilitate speciation if the boreal-adapted peripheral population that crossed the Bering land bridge becomes isolated from those on its original

continent. In addition to the implications they provide for Quaternary biogeography, our findings have important taxonomic implications, including evidence that supports reinstating the previous species-level designation of *Vulpes fulva* for the North American red fox.

Acknowledgements

Thank you to A. Statham for assistance with sampling, and to S. Watanabe and M. Kato for laboratory assistance. The following individuals allowed us access to museum samples: R. Fisher and S. Peurach (National Museum of Natural History) and K. Zyskowski (Peabody Museum of Natural History, Yale University). We would like to thank the following individuals and organizations for providing modern genetic samples: C. O'Reilly (Waterford Institute of Technology, Ireland); D. O'Mahony (Ecological Management Group, Belfast, Northern Ireland); E. Geffen (Tel Aviv University, Israel); S. Lapidge and contributors to the Australian Fox DNA project; R. Wayne (UCLA); K. Norén (University of Stockholm); L. Dalén (Swedish Museum of Natural History, Stockholm); Beringia 2005 expedition organized by the Swedish Polar Research Secretariat; A. Ardalan (Royal Institute of Technology, Stockholm, Sweden); C. Hammar (Al Wabra Wildlife Preservation, Shahaniya, Qatar); R. Kasten and B. Chomel (UC Davis); T. McCarthy (Panthera and Snow Leopard Trust); S. Rabinowitz, I.M.G. Dias, S. Loss (American Museum of Natural History); L. Waits (University of Idaho); M. Abdel (University of Granada); M. Galiana García, J. Carranza and D. Camps Munuera (Spain); T. Bailey (U.A.E.); K. Jumabaev (Kyrgyzstan); D. Ehrich (University of Tromsø, Norway); A. Kukekova (University of Illinois at Urbana-Champaign); and N. Illarionova (Russian Federation). We thank B. Moore (UC Davis) for help with the long tree problem in MrBayes. We thank C. Schrago (Universidade Federal do Rio de Janeiro) for providing time estimate data on divergence of Canids. We thank B. Carstens (Ohio State University) for help and discussion regarding the species delimitation program SpedeSTEM. We thank S. Ho (University of Sydney) for advice regarding Beast. Lastly, we thank five anonymous reviewers whose comments and suggestions on a previous draft greatly improved the quality of this manuscript. Partial funding was provided by the Veterinary Genetics Laboratory at the University of California, Davis, and the Systematics Research Fund (the Systematics Association and the Linnean Society of London).

References

Anderson PH, Lozhkin AV (2001) The Stage 3 interstadial complex (Karginskii/middle Wisconsinan interval) of Beringia: variations in paleoenvironments and implications for paleoclimatic interpretations. *Quaternary Science Reviews*, **20**, 93–125.

Aubry KB (1983) *The Cascade red fox: distribution, morphology, zoogeography and ecology*. PhD Dissertation, University of Washington, Seattle, Washington, USA. 151 pp.

Aubry KB, Statham MJ, Sacks BN, Perrine JD, Wisely SM (2009) Phylogeography of the North American red fox: vicariance in Pleistocene forest refugia. *Molecular Ecology*, **18**, 2668–2686.

Bandelt HJ, Forster P, Röhl A (1999) Median-joining networks for inferring intraspecific phylogenies. *Molecular Biology and Evolution*, **16**, 37–48.

Bugno-Poniewierska M, Sojecka A, Pawlina K, Jakubczak A, Jeżewska-Witkowska G (2012) Comparative cytogenetic analysis of sex chromosomes in several Canidae species using Zoo-FISH. *Folia Biologica*, **60**, 1–2.

Chambers SM, Fain SR, Fazio B, Amaral M (2012) An account of the taxonomy of North American wolves from morphological and genetic analyses. *North American Fauna*, **77**, 1–67.

Churcher CS (1959) The specific status of the New World red fox. *Journal of Mammalogy*, **40**, 349–360.

Culver M, Johnson WE, Pecon-Slattery J, O'Brien SJ (2000) Genomic ancestry of the American puma (*Puma concolor*). *Journal of Heredity*, **91**, 186–197.

Davison J., Ho SYW, Bray SC *et al.* (2011) Late-Quaternary biogeographic scenarios for the brown bear (*Ursus arctos*), a wild mammal model species. *Quaternary Science Reviews*, **30**, 418–430.

Dawson NG, Cook JA (2012) Behind the genes: diversification of North American martens (*Martes americana* and *M. caurina*). In: *Biology and Conservation of Martens, Sables, and Fishers: A New Synthesis* (eds Aubry KB, Zielinksi WJ, Raphael MG, Proulx G, Buskirk SW), pp. 23–38. Cornell University Press, Ithaca, New York, USA.

Desmarest AG (1820) *Mammalogie, ou, description des espèces de mammiféres*. vol. **1**, Veuve Agasse, Paris, 556pp.

Drummond AJ, Rambaut A (2007) BEAST: Bayesian evolutionary analysis by sampling trees. *BMC Evolutionary Biology*, **7**, 214.

Drummond AJ, Rambaut A, Shapiro B, Pybus OG (2005) Bayesian coalescent inference of past population dynamics from molecular sequences. *Molecular Biology and Evolution*, **22**, 1185–1192.

Drummond AJ, Ho SWY, Rawlence N, Rambaut A (2007) *A Rough Guide to BEAST 1.4*. Software Manual.

Dupanloup I, Schneider S, Excoffier L (2002) A simulated annealing approach to define the genetic structure of populations. *Molecular Ecology*, **11**, 2571–2581.

Edwards CJ, Soulsbury C, Statham MJ *et al.* (2012) Temporal genetic variation of the red fox, *Vulpes vulpes*, across western Europe and the British Isles. *Quaternary Science Review*, **57**, 95–104.

Excoffier L, Lischer HEL (2010) ARLEQUIN suite ver 3.5: A new series of programs to perform population genetics analyses under Linux and Windows. *Molecular Ecology Resources*, **10**, 564–567.

Excoffier L, Smouse P, Quattro JM (1992) Analysis of molecular variance inferred from metric distances among DNA haplotypes: application to human mitochondrial DNA restriction data. *Genetics*, **131**, 479–491.

Falush D, Stephens M, Pritchard JK (2003) Inference of population structure using multilocus genotype data: linked loci and correlated allele frequencies. *Genetics*, **164**, 1567–1587.

Forster P, Harding R, Torroni A, Bandelt HJ (1996) Origin and evolution of Native American mtDNA variation: a reappraisal. *American Journal of Human Genetics*, **59**, 935–945.

Frati F, Hartl GB, Lovari S, Delibes M, Markov G (1998) Quaternary radiation and genetic structure of the red fox *Vulpes vulpes* in the Mediterranean Basin, as revealed by allozymes and mitochondrial DNA. *Journal of Zoology*, **245**, 43–51.

Fu YX (1997) Statistical Tests of neutrality of mutations against population growth, hitchhiking and background selection. *Genetics*, **147**, 915–925.

Hailer F, Kutschera VE, Hallstrom BM *et al.* (2012) Nuclear genomic sequences reveal that polar bears are an old and distinct bear lineage. *Science*, **336**(6079), 344–347.

Harrison DL, Bates PJJ (1991) *The mammals of Arabia*, 2nd edn. Harrison Zoological Museum, Sevenoaks, UK. 354 pp.

Heled J, Drummond AJ (2010) Bayesian inference of species trees from multilocus data. *Molecular Biological Evolution*, **27**, 570–580.

Hewitt GM (1999) Post-glacial re-colonization of European biota. *Biological Journal of the Linnean Society*, **68**, 87–112.

Hewitt GM (2000) The genetic legacy of the quaternary ice ages. *Nature*, **405**, 907–913.

Hey J, Nielsen R (2007) Integration within the Felsenstein equation for improved Markov chain Monte Carlo methods in population genetics. *Proceedings of the National Academy of Sciences, USA*, **104**, 2785–2790.

vonHoldt BM, Pollinger JP, Earl DA *et al.* (2011) A genome-wide perspective on the evolutionary history of enigmatic wolf-like canids. *Genome Research*, **21**, 1294–1305.

Hughes SS (2012) Synthesis of *Martes* evolutionary history. In: *Biology and Conservation of Martens, Sables, and Fishers: A New Synthesis* (eds Aubry KB, Zielinksi WJ, Raphael MG, Proulx G, Buskirk SW), pp. 3–22. Cornell University Press, Ithaca, New York, USA.

Inoue T, Nonaka N, Mizuno A *et al.* (2007) Mitochondrial DNA phylogeography of the red fox (*Vulpes vulpes*) in northern Japan. *Zoological Science*, **24**, 1178–1186.

Johnson WE, Godoy JA, Palomares F *et al.* (2004) Phylogenetic and phylogeographic analysis of Iberian lynx populations. *Journal of Heredity*, **95**, 19–28.

Kalinowski ST (2005) HP-Rare: a computer program for performing rarefaction on measures of allelic diversity. *Molecular Ecology Notes*, **5**, 187–189.

Kent WJ (2002) BLAT—the BLAST-like alignment tool. *Genome Research*, **12**(4), 656–664.

Korsten M, Ho SYW, Davison J *et al.* (2009) Sudden expansion of a single brown bear maternal lineage across northern continental Eurasia after the last ice age: a general demographic model for mammals? *Molecular Ecology*, **18**, 1963–1979.

Kukekova AV, Trut LN, Oskina IN *et al.* (2007) A meiotic linkage map of the silver fox, aligned and compared to the canine genome. *Genome Resources*, **17**, 387–399.

Kurtén B (1968) *Pleistocene mammals of Europe*. Weidenfeld and Nicolson, London. 317 pp.

Kurtén B, Anderson E (1980) *Pleistocene mammals of North America*. Columbia University Press, New York, USA. 442 pp.

Kutschera VE, Lecomte N, Janke A *et al.* (2013) A range-wide synthesis and timeline for phylogeographic events in the red fox (*Vulpes vulpes*). *BMC Evolutionary Biology*, **13**, 114.

Larivière S, Pasitschniak-Arts M (1996) *Vulpes vulpes*. *Mammalian Species*, **537**, 1–11.

Leonard JA, Vila C, Wayne RK (2005) Legacy lost: genetic variability and population size of extirpated US grey wolves (*Canis lupus*). *Molecular Ecology*, **14**, 9–17.

Lessa EP, Cook JA, Patton JL (2003) Genetic footprints of demographic expansion in North America, but not Amazonia, during the Late Quaternary. *Proceedings of the National Academy of Sciences, USA*, **100**, 10331–10334.

Librado P, Rozas J (2009) DNASP v5: A software for comprehensive analysis of DNA polymorphism data. *Bioinformatics*, **25**, 1451–1452.

Lloyd HG (1980) *The red fox*. B.T. Batsford Ltd., London, UK. 320 pp.

Macdonald DW, Reynolds JC (2004) Red fox (*Vulpes vulpes*). In: *Canids: Foxes, Wolves, Jackals and Dogs. Status Survey and Conservation Action Plan*. IUCN/SSC Canid Specialist Group. (eds Sillero-Zubiri C, Hoffmann M, Macdonald DW), pp. 129–137. Gland, Switzerland and Cambridge, UK.

Marmi J, López-Giráldez F, Macdonald DW, Calafell F, Zholnerovskaya E, Domingo-Roura X (2006) Mitochondrial DNA reveals a strong phylogeographic structure in the badger across Eurasia. *Molecular Ecology*, **15**, 1007–1020.

Mayr E (1954) Change of genetic environment and evolution. In: *Evolution as a Process* (ed. Huxley J), pp. 157–180. Allen & Unwin, London, UK.

McKelvey KS, Aubry KB, Anderson NJ *et al.* (2014) Recovery of Wolverines in the Western United States: recent extirpation and re-colonization or range retraction and expansion? *The Journal of Wildlife Management*, **78**, 325–334.

Mercure A, Ralls K, Koepfli KP, Wayne RK (1993) Genetic subdivisions among Small Canids: mitochondrial DNA differentiation of Swift, Kit, and Arctic Foxes. *Evolution*, **47**, 1313–1328.

Natanaelsson C, Oskarsson MCR, Angleby H, Lundeberg J, Kirkness E, Savolainen P (2006) Dog Y chromosomal DNA sequence: identification, sequencing and SNP discovery. *BMC Genetics*, **7**, 45.

Norén K, Carmichael L, Dalén L *et al.* (2011) Arctic fox *Vulpes lagopus* population structure: circumpolar patterns and processes. *Oikos*, **120**, 873–885.

Perini FA, Russo CAM, Schrago CG (2010) The evolution of South American endemic canids: a history of rapid diversification and morphological parallelism. *Journal of Evolutionary Biology*, **23**, 311–322.

Perrine JD, Pollinger JP, Sacks BN, Barrett RH, Wayne RK (2007) Genetic evidence for the persistence of the critically endangered Sierra Nevada red fox in California. *Conservation Genetics*, **8**, 1083–1095.

Péwé TL, Hopkins DM (1967) Mammal remains of pre-Wisconsin age in Alaska. In: *The Bering Land Bridge* (ed. Hopkins DM), pp. 266–287. Stanford University Press, Palo Alto, California.

Pinsof JD, Stewart KM, Seymour KL (1996) Current status of North American Sangamonian local faunas and vertebrate taxa. In: *Palaeoecology and Palaeoenvironments of Late Cenozoic Mammals: Tributes to the Career of C.S. (Rufus) Churcher* (eds Stewart KM, Seymour KL), pp. 156–190. University of Toronto Press, Ontario, Canada.

Posada D (2008) jModelTest: Phylogenetic model averaging. *Molecular Biology and Evolution*, **25**, 1253–1256.

Pritchard JK, Stephens M, Donnelly P (2000) Inference of population structure using multilocus genotype data. *Genetics*, **155**, 945–959.

Rambaut A, Drummond AJ (2007) *Tracer v1.5*, Available from http://beast.bio.ed.ac.uk/Tracer.

Randi E (2010) Wolves in the Great Lakes region: a phylogeographic puzzle. *Molecular Ecology*, **19**, 4386–4388.

Ronquist F, Huelsenbeck JP (2003) MrBayes 3: Bayesian phylogenetic inference under mixed models. *Bioinformatics*, **19**, 1572–1574.

Rueness EK, Asmyhr MG, Sillero-Zubiri C *et al.* (2011) The cryptic African wolf: *Canis aureus lupaster* is not a golden jackal and is not endemic to Egypt. *PLoS One*, **6**, e16385.

Sacks BN, Louie S (2008) Using the dog genome to find SNPs in red foxes and other distantly related members of the Canidae. *Molecular Ecology Resources*, **8**, 35–49.

Sacks BN, Statham MJ, Perrine JD, Wisely SM, Aubry KB (2010) North American montane red foxes: expansion, fragmentation, and the origin of the Sacramento Valley red fox. *Conservation Genetics*, **11**, 1523–1539.

Sacks BN, Moore MJ, Statham M, Wittmer HU (2011) A restricted hybrid zone between native and introduced red fox (*Vulpes vulpes*) populations suggests reproductive barriers. *Molecular Ecology*, **20**, 326–341.

Sacks BN, Brown SK, Stephens D, Pedersen NC, Wu JT, Berry O (2013) Y chromosome analysis of dingoes and Southeast Asian village dogs suggests a Neolithic continental expansion from Southeast Asia followed by multiple Austronesian dispersals. *Molecular Biology and Evolution*, **30**, 1103–1118.

Saillard J, Forster P, Lynnerup N, Bandelt H-J, Nørby S (2000) mtDNA variation among Greenland Eskimos: the edge of the Beringian expansion. *American Journal of Human Genetics*, **67**, 718–726.

Schipper J, Chanson JS, Chiozza F *et al.* (2008) The Status of the World's land and Marine Mammals: diversity, threat, and knowledge. *Science*, **322**, 225–230.

Shapiro B, Rambaut A, Drummond AJ (2006) Choosing appropriate models for the phylogenetic analysis of protein-coding sequences. *Molecular Biology and Evolution*, **23**, 7–9.

Sharma DK, Maldonado JE, Jhala YV, Fleischer RC (2004) Ancient wolf lineages in India. *Proceedings of the Royal Society B*, **271**, S1–S4.

Shrotriya S (2012) Wolves in Trans-Himalayas: 165 years of taxonomic confusion. *Current Science*, **103**, 885–887.

Stamatakis A (2006) RAxML-VI-HPC: Maximum likelihood-based phylogenetic analyses with thousands of taxa and mixed models. *Bioinformatics*, **22**, 2688–2690.

Statham MJ, Trut LN, Sacks BN *et al.* (2011) On the origin of a domesticated species: identifying the parent population of Russian silver foxes (*Vulpes vulpes*). *Biological Journal of the Linnean Society*, **103**, 168–175.

Statham MJ, Rich AR, Lisius SK, Sacks BN (2012a) Discovery of a remnant population of Sierra Nevada red fox (*Vulpes vulpes necator*). *Northwest Science*, **86**, 122–132.

Statham MJ, Sacks BN, Aubry KB, Perrine JD, Wisely SM (2012b) The origin of recently established red fox populations in the contiguous United States: translocations or natural range expansions? *Journal of Mammalogy*, **93**, 52–65.

Tajima F (1989) Statistical method for testing the neutral mutation hypothesis by DNA polymorphism. *Genetics*, **123**, 585–595.

Teacher AGF, Thomas JA, Barnes I (2011) Modern and ancient red fox (*Vulpes vulpes*) in Europe show an unusual lack of geographical and temporal structuring, and differing responses within the carnivores to historical climatic change. *BMC Evolutionary Biology*, **11**, 214.

Toews DP, Brelsford A (2012) The biogeography of mitochondrial and nuclear discordance in animals. *Molecular Ecology*, **21**, 3907–3930.

Vila C, Amorim IR, Leonard JA *et al.* (1999) Mitochondrial DNA phylogeography and population history of the grey wolf *Canis lupus*. *Molecular Ecology*, **8**, 2089–2103.

Weckworth BV, Talbot SL, Cook JA (2010) Phylogeography of wolves (*Canis lupus*) in the Pacific Northwest. *Journal of Mammalogy*, **91**, 363–375.

Williams JB, Muñoz-Garcia A, Ostrowski S, Tieleman BI (2004) A phylogenetic analysis of basal metabolism, total evaporative water loss, and life-history among foxes from desert and mesic regions. *Journal of Comparative Physiology, B.*, **174**, 29–39.

Wilson PJ, Grewal SK, Lawford ID *et al.* (2000) DNA profiles of the eastern Canadian wolf and the red wolf provides evidence for a common evolutionary history independent of the gray wolf. *Canadian Journal of Zoology*, **78**, 2156–2166.

Woerner AE, Cox MP, Hammer MF (2007) Recombination-filtered genomic datasets by information maximization. *Bioinformatics*, **23**, 1851–1853.

Appendix I

Museum identification numbers for red fox specimens where DNA was extracted specifically for this study. Specimens that did not provide any usable DNA are marked with the letter code 'f'. All other samples provided sequence data.

Harrison Institute, Kent, UK. 4.1976, 5.1977, 6.1978, 7.1979, 8.1980, 9.1981, 10.3177, 13.3727, 14.3734 f, 15.3860, 16.3993, 17.4108, 18.4109, 19.4110, 20.4111, 22.4113, 23.4360, 25.4530, 26.4547, 27.4549, 28.4550, 35.8139, 36.8273, 37.8325, 38.8598, 39.8620, 40.9123, 42.10047, 45.11174, 48.11646, 49.12339, 52.17445, 60.25113, 61.25114, 62.25115, 63.25225.

Harvard Museum of Comparative Zoology, Cambridge, Massachusetts, USA. BOM7081, MCZ13680, MCZ14444 f, MCZ14445, MCZ15722, MCZ16701, MCZ16705, MCZ23946 f, MCZ23948, MCZ23949, MCZ24837, MCZ24865, MCZ49029, MCZ49030, MCZ51297 f, MCZ51511, MCZ51516, MCZ6469 f, MCZ8609, MCZ8612, MCZ8740, MCZ8909, MCZ8911, MCZ8914.

Natural History Museum, Cromwell Road, London, UK. NHM 1851.4.23.14, NHM1856.3.12.14, NMH1859.12.3.1, NMH 1879.11.21.538 f, NMH1881.8.16.7, NMH 1881.8.16.8, NMH 1885.8.1.58 f, NMH1885.8.1.64, NMH1886.5.6.2 f, NMH1892.7.15.3 f, NMH1897.3.12.5 f, NMH1898.7.4.8 f, NMH1901.5.5.23 f, NMH1903.2.8.9, NMH1904.8.2.19, NMH1907.4.3.7 f, NMH1915.11.1.77, NMH1915.11.1.78, NMH1919.11.8.10, NMH1919.8.19.2, NMH1919.9.20.4, NMH1919.9.20.5, NMH1926.10.8.34 f, NMH1939.1728 f, NMH1939.858, NMH1943.212, NMH1947.1408, NMH1965.1038,

NMH1966.173 f, NMH1978.26 f, NMH1978.27, NMH1978.28, NMH1978.29, 176c.

Yale Peabody Museum of Natural History, New Haven, Connecticut, USA. YPM 3335 f, YPM3336 f, YPM3337 f, YPM10264, YPM 10423, YPM2221, YPM2872, YPM3410, YPM3411, YPM3412, YPM3413, YPM3414.

National Museum of Natural History, Washington, D.C. USA. USNM201068.

M.J.S. conceived the study, generated data, and conducted analyses. M.J.S. and B.N.S. designed the study, gathered samples, and wrote the paper. K.B.A., O.B., J.J. and J.M. assisted with editing the manuscript. J.M., J.J., O.B. and all other authors provided samples and/or genetic data, discussed results, and contributed to writing the paper.

Data accessibility

All mtDNA data generated, alignment of all mtDNA haplotypes, all cytochrome *b* and D-loop haplotypes combinations, autosomal sequence data and associated Y-chromosome and mtDNA haplotypes, linked Y-chromosome alleles, *Beast input file and tree files for Beast and MrBayes are available at DRYAD entry doi:10.5061/dryad.4g5gb.

Supporting information

Additional supporting information may be found in the online version of this article.

Appendix S1 Taxonomic History of North American Red Fox.

Appendix S2 Use of root and tip approaches to dating mtDNA clades.

Appendix S3 Estimation of splitting times between continental red foxes.

Appendix S4 Detailed description of red fox subclades in this study.

Appendix S5 Detailed description of Eurasian red fox population differentiation.

Table S1 List of geographic areas sampled and the number of samples from each area included in genetic analyses for each marker type.

Table S2 Red fox Y-chromosome microsatellite locus information.

Table S3 Times to most recent common ancestor (TMRCA) of red fox mtDNA clades and subclades based on rho analyses, using a fixed mutation rate as described in the main text.

Table S4 Mitochondrial DNA splitting time and demographic analyses of red fox populations on either side of the Bering Strait in Eurasia/Africa and North America.

Table S5 Pairwise estimates of F_{ST} of red foxes from six large geographic regions based on eleven nuclear gene sequences.

Table S6 Global red fox mtDNA diversity and neutrality statistics based on concatenated cytochrome *b* and D-loop sequences.

Figure S1 Phylogenetic tree including time estimates of red fox mtDNA groups.

Figure S2 Phylogenetic tree with partitioning beyond the clade level.

Figure S3 Haplotype networks of the two main nested red fox mtDNA clades and the Palearctic basal haplotypes.

Figure S4 Haplotype networks for 11 nuclear gene regions. Each network represents up to 108 fox nuclear haplotypes; 102 from red fox and 6 from other *Vulpes* species.

Figure S5 Unrooted neighbor-joining tree of 36 red fox sampling sites.